Effects of Periodic Wake Passing upon Flat-Plate Boundary Layers Experiencing Favorable and Adverse Pressure Gradient

Ken-ichi Funazaki and Eitaro Koyabu
Department of Mechanical Engineering
Iwate University
Morioka, Japan

ABSTRACT

This paper deals with the investigation of wake-disturbed boundary layer on a flat-plate model with an elliptic leading edge. The wakes are generated by the transversely moving bars in front of the test model. Main focus of this paper is on how the wake passage affects the transitional behavior of the boundary layer under the influence of favorable and adverse pressure gradients over the test surface. Detailed measurements of the boundary layer are conducted by use of a hot-wire anemometry. An ensemble-averaging technique is also employed in order to extract the periodic events associated with the wake passage from the acquired data. It follows that a salient difference in wake-induced transition of the boundary layer is confirmed between two opposing cases in terms of the direction of the wake-generating bar movement. It is also found that the wake passage induces a significant change in the flow structure downstream of the end of the flow acceleration.

NOMENCLATURE

d	: diameter of the wake-generating bar
C_p	: pressure coefficient
$\tilde{f}$	: wake passing frequency
$\tilde{H}_{12}$	: shape factor
L	: length of the test model
n	: number of rotation
n_b	: number of wake-generating bar
Re	: Reynolds number (= $U_\infty L/\nu$)
Re_x	: local Reynolds number (= $U_e(x)x/\nu$)
S	: Strouhal number
T	: wake-passing frequency
$\tilde{T}u$	: ensemble-averaged turbulence intensity
T_g	: bulk temperature of the main flow
T_i	: initial temperature of the test model
t	: time
$U_e(x)$	: free-stream velocity at the outer edge of the boundary layer
U_∞	: inlet velocity
$\tilde{v}, v_k$	: ensemble-averaged velocity, sampled velocity data
x	: streamwise coordinate
y	: distance from the surface of the test model

Greeks

δ_{99}	: boundary layer thickness
$\tilde{\delta}$	: boundary layer thickness
δ_1	: displacement thickness
ν	: kinematic viscosity
ρ	: density

Superscript

~	: ensemble-averaged value

INTRODUCTION

A number of concerns have been raised about the unsteady-flow effect on the aerodynamic performance of rotor and/or stator cascades of axial turbomachines. For example, the deterioration in aerodynamic performance of a low-pressure turbine stage in commercial aero-engines, which is anticipated to occur when they operate under the cruise condition, could be reduced due to the existence of wake-blade interaction. Shulte and Hodson (1994)(1996)) found from the inspection of the steady and wake-affected pressure distributions on the blade suction surface that upstream blade wakes seemingly suppressed a separation bubble which would otherwise occurred on the suction surface and deteriorated the cascade performance. Besides, Funazaki et al. (1997c) conducted the measurement of stagnation pressure distributions downstream of a linear cascade of turbine blades that was subjected to periodic wakes from the upstream moving bars. Funazaki et al. accordingly identified a considerable reduction in the loss associated with the blade wake. Likewise in the study of Shulte and Hodson, they concluded from the flow visualization that a separation bubble on the blade suction surface was almost diminished due to the wake-blade interaction. Halstead et al. (1995a)(1995b) investigated the wake-blade interaction phenomena in a large-scale compressor and a turbine. Fundamental studies on separation bubble were reported by several researchers as well.

Despite the above-mentioned studies, information is still lacking on the effects of free-stream turbulence and periodic wake passage upon the behavior of the separation bubble over a blade surface, which is indispensable for the development of more efficient turbomachines. At the same time, such an information is strongly needed for the verification of CFD codes as well as turbulence models that will be used in the aerodynamic design. This has driven the authors to start a research project which aims to gain quantitative

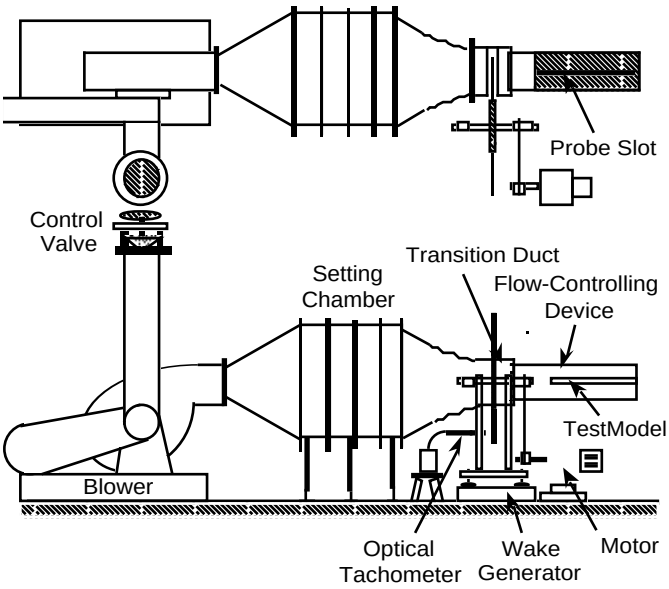

Figure 1 Test apparatus

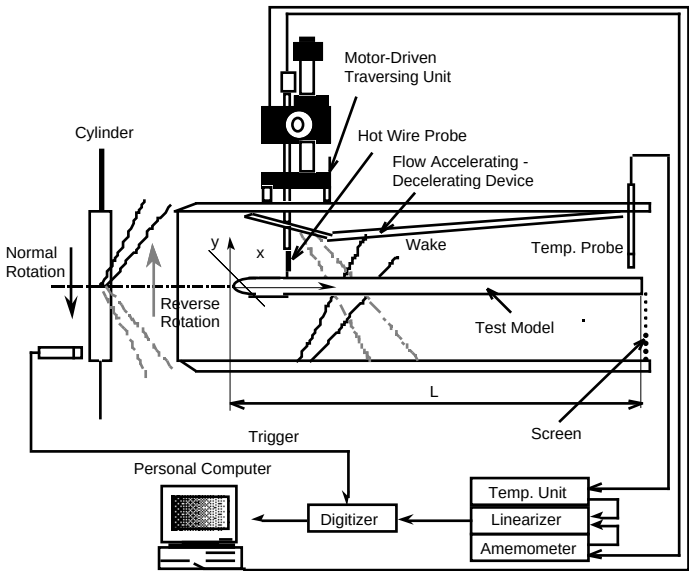

Figure 2 Test model and the system for boundary layer measurement, with an explanatory illustration of wakes generated in the normal and reverse rotations

data of the aerodynamic interaction between the separation bubble and incoming periodic wakes and/or free-stream turbulence. This paper describes the relevant fundamental studies employing a flat plate with an elliptic leading edge as a test model instead of a real turbine blade, in which the wake-affected boundary layer experiencing favorable and then adverse pressure gradient was investigated in detail. A focus was placed on how the periodic wake passage influenced the behavior of the boundary layer at the region where a separation bubble was likely to occur. A duct-contouring device was adopted to adjust the pressure gradient so that the pressure gradient of the turbine blade used by Funazaki et al. (1997c) was emulated over the test surface. A spoked-wheel type wake generator was employed to generate incoming wakes. This study also examined the effect of the rotation direction of the wake generator upon the aerodynamic interaction between the wakes and the boundary layer likewise in the previous studies (Funazaki et al. (1997a)(1997b)). Detailed hot-wire probe measurements were executed to obtain steady and wake-affected velocity data of the boundary layer.

TEST APPARATUS

Experimental Setup

Figure 1 shows a schematic layout of the test facility used in this study. The settling chamber and the contraction nozzle reduced free-stream turbulence from the blower down to about 0.8%. Incoming wakes were produced by a spoked-wheel type wake generator which was located upstream of the test model. The wake generator consisted of a disk with 400mm diameter and cylindrical bars of 5mm diameter. Revolution number of the disk in the wake generator was counted by the optical tachometer. The fluctuation in revolution was also monitored and it was found to be less than 0.5%. Figure 2 shows the test model and the passage-contouring device attached on the top wall of the test duct which was used to realize a specified pressure gradient on the surface of the test model. Also shown is the system for the boundary layer measurement. The test model made of acrylic-resin had a semi-elliptic leading edge with the long axis of 75mm and the short axis of 30mm, followed by a flat-plate afterbody. Static pressure taps were provided on one side of the test model to measure the pressure distribution imposed on the test surface. Stainless steel foils covered the other side of the model to measure wake-affected heat transfer on the surface, which was not reported in this study. The passage-contouring device was adjusted so as to reproduce the pressure distribution similar to that on the suction surface of the turbine blade which was investigated by Funazaki et al. (1995a). In order to avoid a biased inflow condition due to the asymmetric configuration of the test model with respect to the duct center line, a screen was attached to the lower exit of the test duct. The mesh size of the screen was selected so that the aerodynamic stagnation line almost match the mechanical stagnation line, which was confirmed by the oil-flow pattern near the leading edge of the test model. The contouring device was equipped with a slot along its center line through which a hot-wire probe could be inserted into the main flow. The slot was securely plugged with several acrylic-resin blocks to prevent the leakage from the slot.

Revolution direction of the disk in the wake generator was easily switched, which changed the relative movement of the wake-generating bars against the test model, as designated 'normal rotation' or 'reverse rotation' in Figure 2. Funazaki et al. (1996a)(1996b) found through the previous studies that the relative movement of the bars and the associated fluid motion so-called negative jet seemed to have some effects on the transitional behavior of the wake-affected boundary layer. In those cases, however, since the leading edge of the test model used was sharp-edged, it could not be completely denied that the sharp-edged leading edge affected the transitional behavior of the boundary layer through the temporal fluctuation of the flow incidence associated with the wake passing. Therefore, the present study was anticipated to yield another evidence for the negative-jet effect upon the wake/boundary layer interaction.

Instrumentation and Data Processing

A single hot-wire probe was used to measure the boundary layer on the test model. A PC-controlled traversing unit precisely placed the probe to the location to be measured. The probe was connected to a constant temperature anemometer. By monitoring the free-stream temperature at the exit of the test section, T_∞, the temperature unit effectively compensated the temperature fluctuation of relatively low frequency during the long-running measurement. A/D conversion of the linearized signal of the probe was initiated with once-per-revolution signal from the optical tachometer, which guaranteed the application of the phase-locked averaging technique to the sampled data. Data sampling rate was 50kHz and each of the digitized time-history records contained 2048 words. Accordingly,

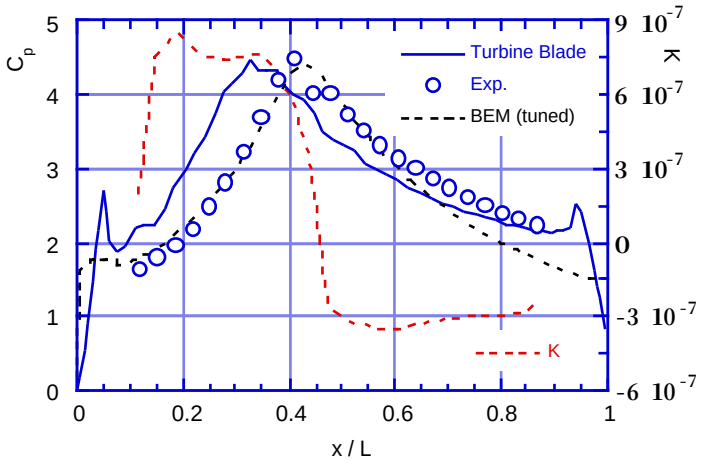

Figure 3 Measured and calculated pressure distributions over the test surface, in comparison with the target pressure distribution on the turbine blade suction surface

phase-locked or ensemble-averaged velocity, $\tilde{v}$ was calculated from the acquired instantaneous velocity data, v_k (k =1,2,...,100) as follows:

$$\tilde{v}(x,y,t)=\frac{1}{N}\sum_{k=1}^{N}v_k(x,y,t) \qquad (1)$$

Ensemble-averaged turbulence intensity was also defined by

$$\tilde{T}u(x,y,t)=\frac{1}{U_e(x)}\sqrt{\frac{1}{N-1}\sum_{k=1}^{N}\left(v_k(x,y,t)-\tilde{v}(x,y,t)\right)^2}\ , \qquad (2)$$

where U_e was the local velocity determined from the static pressure measurements with the Bernoulli's equation. From the ensemble-averaged velocity, boundary layer integral characteristics such as displacement thickness could be calculated using the following equations:

$$\tilde{\delta}_1(x,t)=\int_0^{\tilde{\delta}(x,t)}\left(1-\frac{\tilde{v}(x,y,t)}{U_e(x)}\right)dy\ , \qquad (3)$$

$$\tilde{\delta}_2(x,t)=\int_0^{\tilde{\delta}(x,t)}\left(1-\frac{\tilde{v}(x,y,t)}{U_e(x)}\right)\frac{\tilde{v}(x,y,t)}{U_e(x)}dy\ . \qquad (4)$$

$\tilde{\delta}$ was an ensemble-averaged boundary layer thickness, which was the distance where the ensemble-averaged velocity reached the maximum among the data acquired at the same streamwise location. Shape factor was accordingly calculated by

$$\tilde{H}_{12}(x,t)=\tilde{\delta}_1(x,t)/\tilde{\delta}_2(x,t)\ . \qquad (5)$$

RESULTS

Test Conditions

Wake-affected unsteady flow field around the test model was characterized by two non-dimensionalized number, i.e., Reynolds number Re, and Strouhal number S, defined by

$$Re=\frac{U_\infty L}{\nu} \qquad (6)$$

$$S=\frac{fL}{U_\infty}=\frac{nn_b}{60}\frac{L}{U_\infty} \qquad (7)$$

where U_∞ was inlet velocity and L was the length of the test model (= 1.075 m). In the present case U_∞ was 20 m/s, n was 1200 rpm and n_b was 2, 3 or 6, corresponding to $Re\cong 1.43\times10^6$ and S =2.15, 3.23 or 6.45, respectively.

Static Pressure Distribution

Figure 3 shows the pressure distribution on the suction surface of the turbine blade used by Funazaki et al. (1997c) and the measured static pressure distribution, with the calculated one by use of a BEM-based potential flow analysis code for comparison. In this case static pressure coefficient, C_p is calculated by

$$C_p=\frac{P_0-p}{1/2\rho U_\infty^2}=\left(U_e/U_\infty\right)^2\ . \qquad (8)$$

Also shown is the corresponding acceleration parameter defined by the following equation:

$$K=\frac{\nu}{U_e^2}\frac{dU_e}{dx}\ . \qquad (9)$$

It follows that the average acceleration parameter was about 0.8×10^{-6} before the deceleration. Although a slight difference in the peak position of the pressure distribution was observed between the two cases for the turbine blade and the present test model, the overall profiles of the pressure distributions was similar to each other. Figure 3 also exhibits a small plateau just downstream of the peak value in the measured pressure distribution, implying the existence of a separation bubble.

Time-Resolved Behaviors of the Wake-Affected Boundary layer

Raw Data Figure 4 shows the raw signals of the velocity acquired at $y=0.2\times10^{-3}$ mm for several measurement locations in the case of no wake condition Although each of the measured points located relatively at the different location in the boundary layer, these figures clearly revealed some features of the transitional boundary layer experiencing a favorable and then adverse gradients. Looking into the several velocity data obtained at the location 3 through the location 7 ranging from x/L =0.44 to x/L =0.477, a meaningful decrease in time-averaged velocity was observed at the location 5 (x/L =0.486). This almost matched the pressure data shown in Figure 3, however, the boundary layer was so thin that it was quite difficult to confirm the existence of a possible separation bubble near that region with the present measurement using a single hot-wire probe. Spike-like events occurred at the location 8 indicating the initiation of the transition, followed by the abrupt completion of the transition. Figure 5 shows comparisons of the measured displacement and momentum thicknesses with the calculation using the boundary layer analysis code developed by Schmidt and Patankar (1991). The calculated results almost matched the experimental data except for the location x/L > 0.4, probably due to the insufficiency of the code in dealing with the near-zero shear stress region and its associated transitional flow region.

Figure 6 also exhibits the raw data of the wake-affected velocity in the case of $S=2.15$. Two diagrams are shown for each of the measurement locations, where an upper and a lower diagrams present the data acquired in the normal and reverse rotation cases, respectively. As seen in the diagrams at the location 1, the most upstream measurement point, the wake passage induced contrastive events in the normal and the reverse rotation cases. The detected velocity decreased during the wake passing in the normal rotation case, while

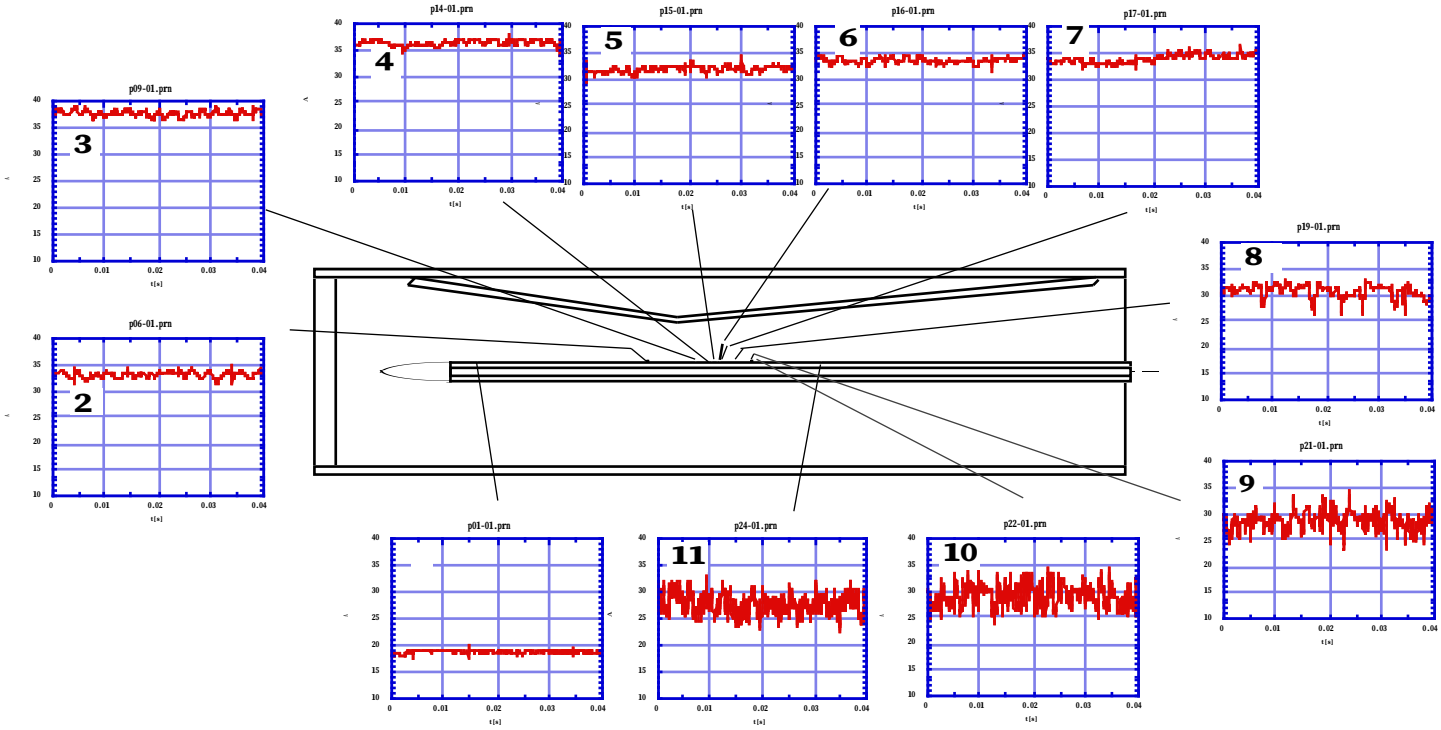

Number	xsurf/L	Number	xsurf/L	Number	xsurf/L	Number	xsurf/L
1	0.144	4	0.463	7	0.477	10	0.523
2	0.375	5	0.468	8	0.495	11	0.606
3	0.440	6	0.472	9	0.514		

L=1.075[m]

Figure 4 Raw velocity signals measured at $y = 0.2 \times 10^{-3}$ for several locations over the test model in the case of no wake condition, showing the transitional behavior of the boundary layer under the influence of the pressure gradient

the velocity in the reverse rotation exhibited slight decrease followed by evident increase. This difference seems to be attributed to an effect of negative jet of the wake which impinges on the test surface in the normal rotation and leave the test surface in the reverse rotation in a relative frame of reference moving with the free-stream. Enlargement of the highly fluctuating regions was observed from the data at the locations 2, 3 and 4, indicating the progress in the wake-induced transition towards the downstream, however, the durations of those regions clearly differ between the normal and reverse rotation cases, as reported in the previous studies by Funazaki et al. (1997a)(1997b). Close inspections of the data revealed that the highly fluctuating regions for the normal rotation case were likely to be accompanied by the significant decrease in velocity, while those regions for the reverse rotation showed only minor velocity decrease. In order to examine these phenomena with the from the viewpoint of the negative jet effect, the study done by Valkov and Tan (1993) was reviewed, who analyzed the wake-disturbed flow field around a compressor cascade by use of a Navier-Stokes solver. Figure 7 shows the disturbance flow vectors around the compressor blade, which were calculated by subtracting the calculated unsteady flow field from the corresponding steady flow field at two different instants. Speaking of the relation of their results to the present study, wakes on the blade suction or pressure surface seemingly corresponded to ones in the reverse rotation case or the normal rotation case from the viewpoint of the relative motion of the fluid inside the wake against the surface of concern. However, one should keep in mind that the pressure distribution on the compressor blade was quite different from the present case, which possibly affected the boundary layer thickness. It was found that incoming wakes were deformed by the

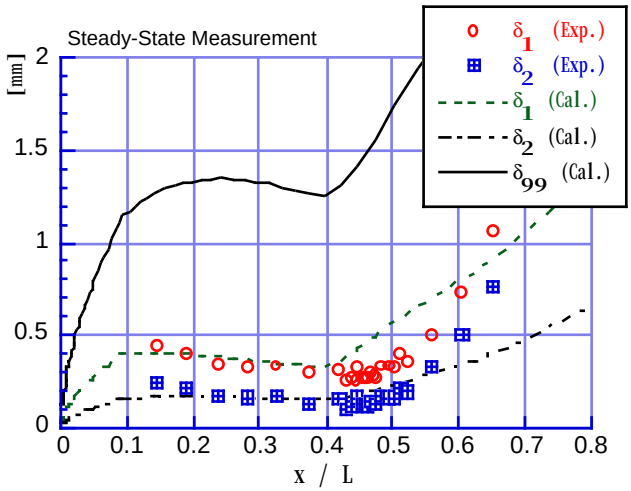

Figure 5 Comparisons of displacement and momentum thicknesses between the measurement and the calculation

stagnant flow at the leading edge, resulting in the appearance of accelerated flow region following the wake as expected from the negative jet theory (see Figure 7(b)). In addition it follows from Figure 7 that the incoming wakes on the suction surface tended to migrate away from the suction surface, in spite of the fact that a numerical viscosity excessively decayed the wakes. Therefore one can conclude that the above-mentioned difference in the duration of the fluctuating region was mainly due to the effect of the wake

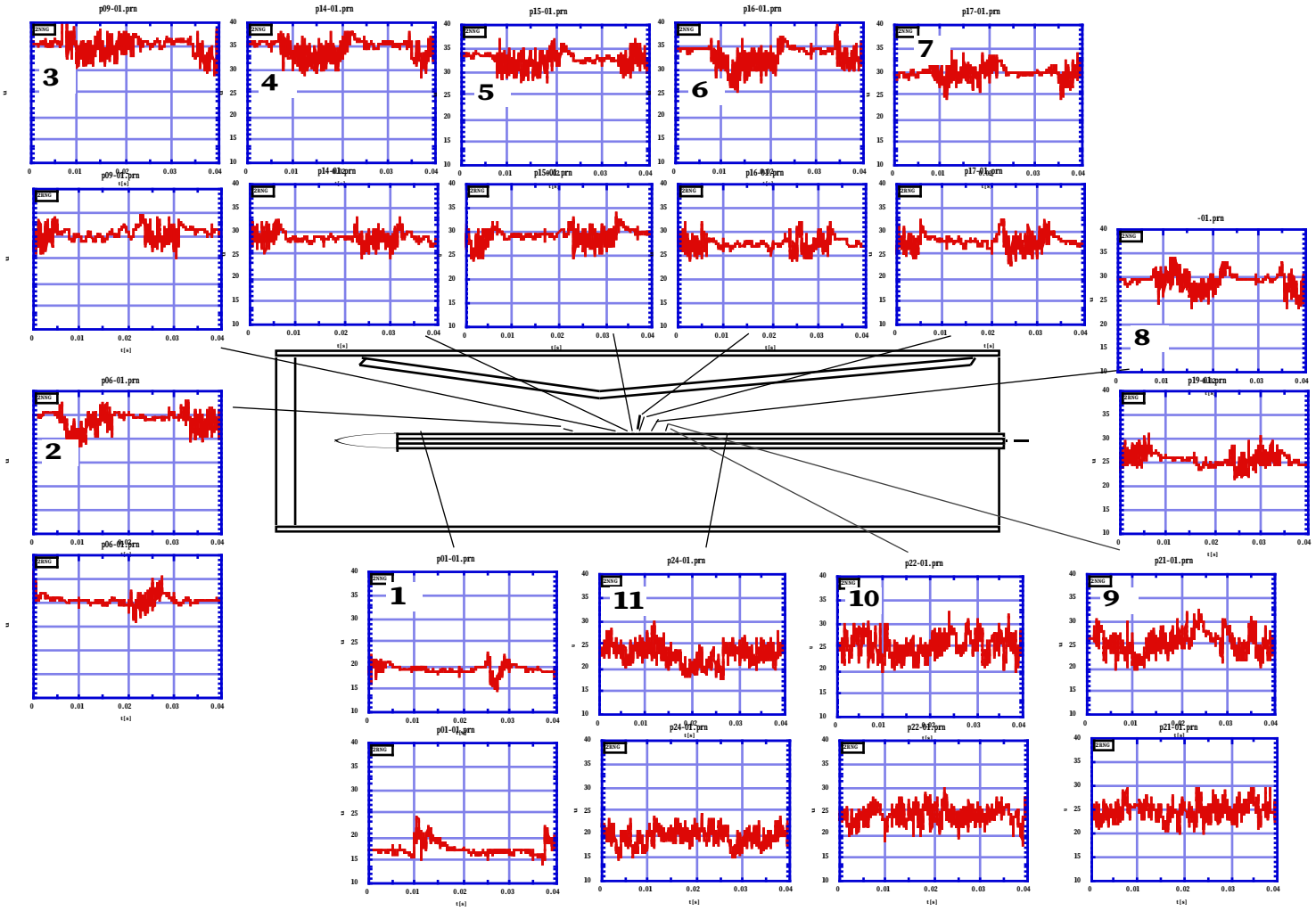

Figure 6 Raw velocity signals measured at $y = 0.2 \times 10^{-3}$ for several locations over the test model with the influence of the wake passing over the test surface ($S = 2.15$), where the upper and lower data of each of the graph columns were acquired in the normal and reverse rotation cases, respectively.

migration from the suction surface. At the location 8 spike-like events were no longer observed and the boundary layer thereafter reached the turbulent state rather abruptly. This observation implies that the wake-induced transition mode dominated the transition process as a whole, assisted by the adverse pressure gradient to become fully turbulent state.

Ensemble-Averaged Turbulence Intensity For further investigation of the wake-affected boundary layer, ensemble-averaged turbulence intensity contours that represent bar-wakes interacting with the boundary layer are shown in Figure 8. This figure represents some of the sequential snapshots during one wake-passing period T for the case of the normal rotation with S =3.23. After one bar-wake, identifiable from its high turbulence intensity reached the most upstream measuring position at $t/T \cong 0.0$, there was a clear evidence showing the appearance of wake-induced turbulence zone (turbulence patch) beneath the incoming wake. As the wake was convected downwards, the leading edge of the induced turbulence patch moved almost along with the wake while the trailing edge of the patch lagged behind the wake, resulting in gradual expansion of the turbulence patch in the streamwise direction. Due to the effect of the flow acceleration, however, the height of the patch remained almost unchanged. In the instant when the leading

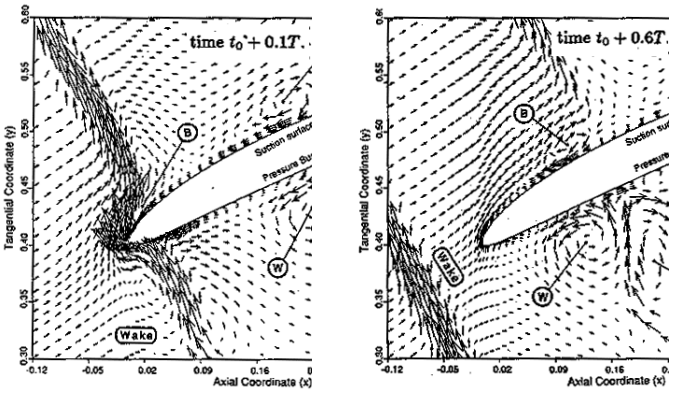

Figure 7 Numerical calculations of wake- compressor blade interaction executed by Valkov and Tan (1983)

edge of the patch reached the trailing edge of the foregoing turbulence patch (t/T =0.4), another high turbulence region occurred at x/L = 0.45 - 0.5 (from location 4 to location 7) designated 'A', exhibiting quick growth in the y-direction (normal to the wall) due to the effect of adverse pressure gradient. A plausible explanation on this event

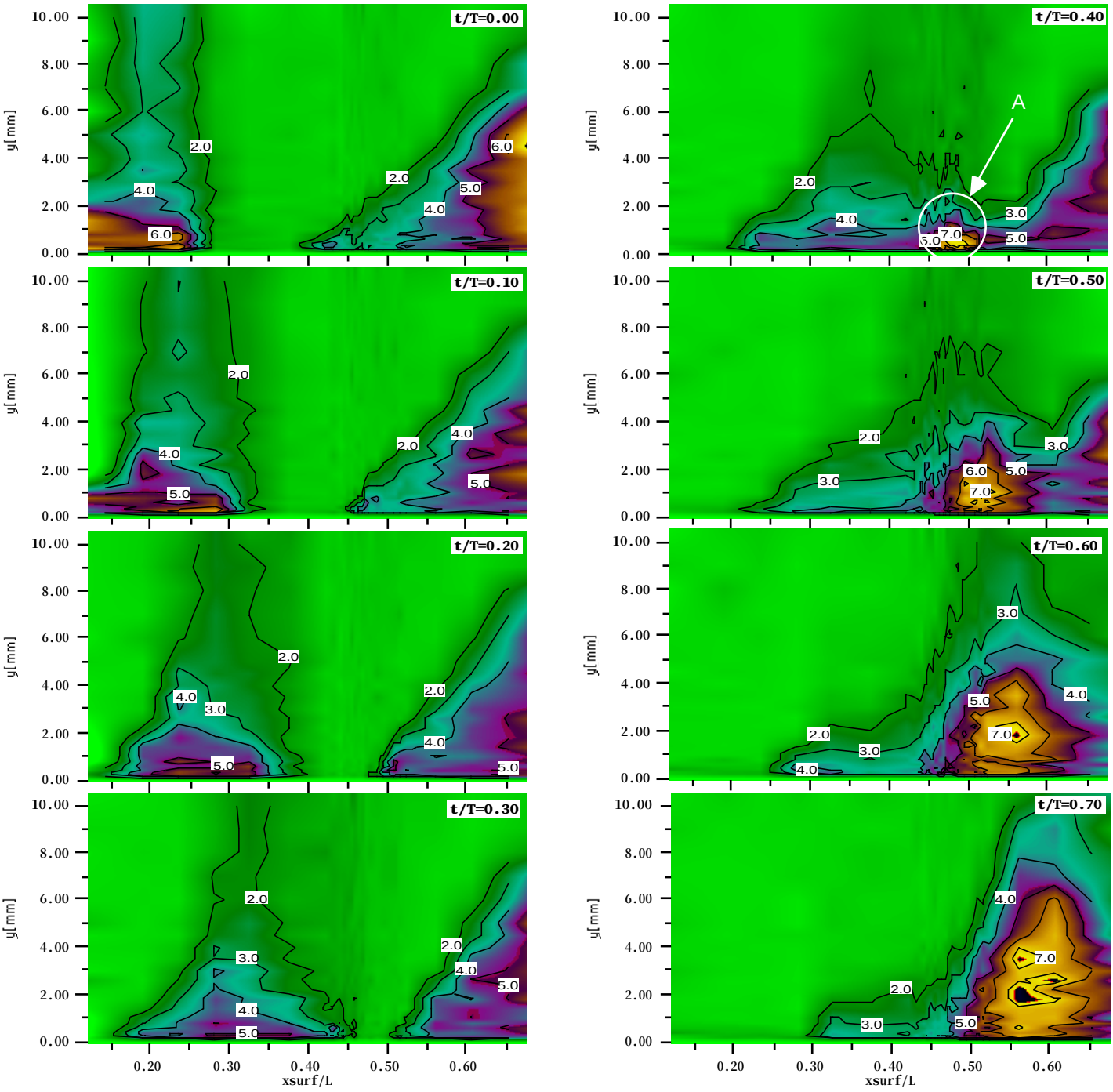

Figure 8 Snapshots of the ensemble-averaged turbulence intensity contours of the wake-disturbed boundary layer experiencing favorable and adverse pressure gradients (S =3.23 / Normal Rotation)

was the interaction between the bar-wake and a possible separation bubble which was not completely confirmed. The other cause was related to a high rate of turbulnce spots generation at the decelerating flow regime (Mayle (1991)).

Figure 9 also shows the snapshots of the ensemble-averaged turbulence intensity contours for the reverse rotation with S =3.23. As seen in the raw data of Figure 5 or numerical calculation in Figure 7, the incoming wake moved away from the test surface so that the wake width (or wake duration) was narrow compared to that of the normal rotation case. Since contributions from the wake turbulence to the turbulence patch was minimal, the streamwise extent of the turbulence patch was also relatively narrow. At the moment when the wake passed over the zone x/L =0.45 - 0.5 , a highly turbulent region designated 'B' appeared and grew likewise in the normal rotation case.

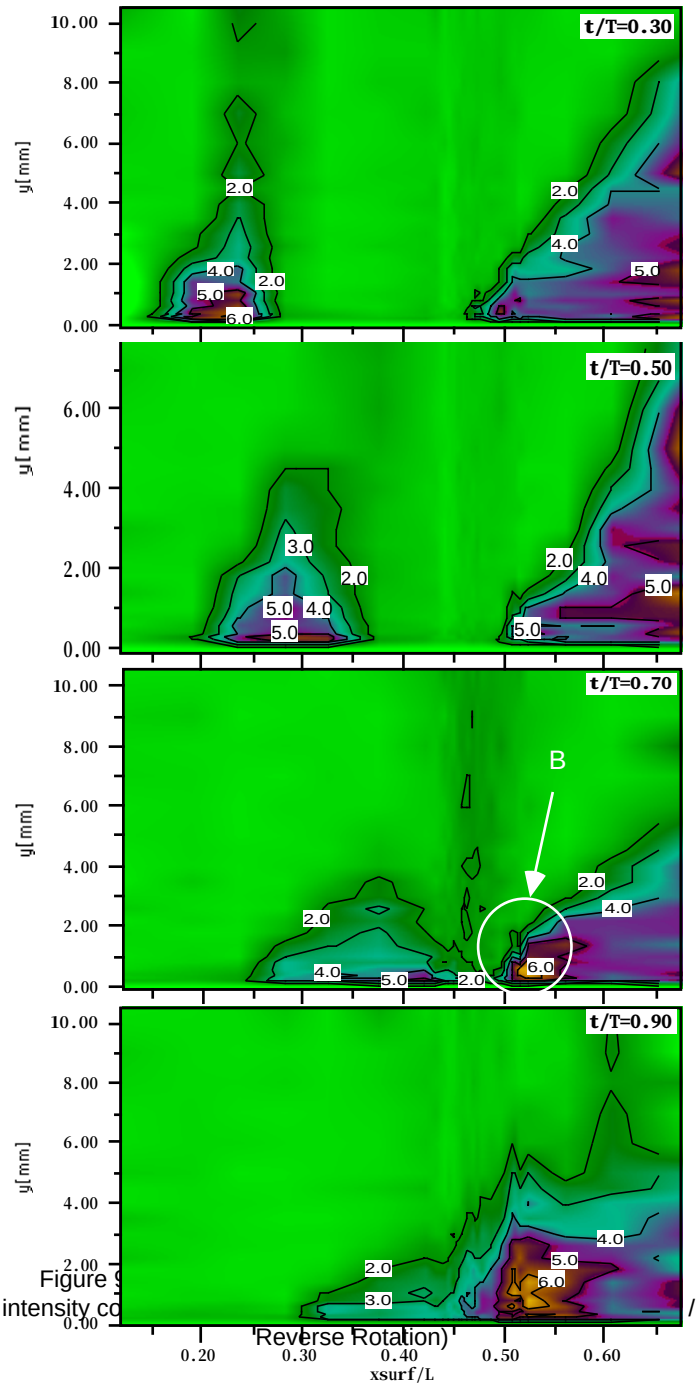

Figure 9
intensity co / Reverse Rotation)

CONCLUSIONS

ACKNOWLEDGMENTS

The authors are greatly indebted to Mr. K. Sasaki of Technical Center of Iwate University in manufacturing the test facility.

REFERENCES

Funazaki, K., 1996a, "Unsteady Boundary Layers on a Flat Plate Disturbed by Periodic Wakes: Part I - Measurement of Wake-Affected Heat Transfer and Wake-Induced Transition Model," Trans. ASME Journal of Turbomachinery, Vol. 118, pp. 327-336.

Funazaki, K., 1996b, "Unsteady Boundary Layers on a Flat Plate Disturbed by Periodic Wakes: Part II - Measurement of Unsteady Boundary Layers and Discussion," Trans. ASME Journal of Turbomachinery, Vol. 118, pp. 337-346.

Funazaki, K., Kitazawa, T., Koizumi, K. and Tanuma, T., 1997a, "Studies on Wake-Disturbed Boundary Layers under the Influences of Favorable Pressure Gradient and Free-Stream Turbulence - Part II : Effect of Free-Stream Turbulence," ASME Paper 97-GT-.

Funazaki, K., Kitazawa, T., Koizumi, K. and Tanuma, T., 1997b, "Studies on Wake-Disturbed Boundary Layers under the Influences of Favorable Pressure Gradient and Free-Stream Turbulence-Part I : Experimental Setup and Discussions on Transition Model," ASME Paper 97-GT-.

Funazaki, K., Sasaki, Y. and Tanuma, T., 1997c, "Experimental Studies on Unsteady Aerodynamic Loss of a High-Pressure Turbine Cascade," ASME Paper 97-GT-.

Funazaki, K., 1995a, "Studies on Wake-Affected Heat Transfer around the Leading Edge of a Blunt Body," ASME/JSME Thermal Engineering Conference., 1, pp. 343 - 350.

Halstead, D. E., Wisler, D. C., Okiishi, T. H., Walker, G. J., Hodson, H. P. and Shin, H. W., 1995a, "Boundary Layer Development in Axial Compressor and Turbines, Part 2 of 4: Compressors," ASME Paper 95-GT-462.

Halstead, D. E., Wisler, D. C., Okiishi, T. H., Walker, G. J., Hodson, H. P. and Shin, H. W., 1995b, "Boundary Layer Development in Axial Compressor and Turbines, Part 3 of 4: LP Turbines," ASME Paper 95-GT-463.

Mayle, R. E., 1991, "The Role of Laminar-Turbulent Transition in Gas Turbine Engines," Trans. ASME Journal of Turbomachinery, Vol. 113, pp. 509-537.

Schmidt, R. C. and Patankar, S. V., 1991, "Simulating Boundary Layer Transition with Low-Reynolds-Number k-e Turbulence Models:Part 1 - An Evaluating of Prediction Characteristics," Trans. ASME Journal of Turbomachinery, Vol. 113, pp. 10-17.

Schulte, V. and Hodson, H. P., 1994, "Wake-Separation Bubble Interaction in Low Pressure Turbines," 30th AIAA/ASME/SAE/ASEE Joint Propulsion Conference.

Schulte, V. and Hodson, H. P., 1996, "Unsteady wake-Induced Boundary Layer Transition in High Lift Turbines," ASME Paper 96-GT-486.

Valkov, T. and Tan, S., 1993, "Control of the Unsteady Flow in a Stator Blade Row Interacting with Upstream Moving Wakes," ASME Paper 96-GT-23.